The Flexible Magnetic Field Thruster

John R. Brophy* and Paul J. Wilbur†
Colorado State University, Fort Collins, Colorado

The flexible magnetic field thruster is a unique research tool for studying the behavior of direct current electron-bombardment ion thrusters. It utilizes a long wire anode shielded by a circumferential magnetic field. The magnetic field around the anode, which is produced by passing a direct current of up to 150 A through the wire, restricts primary electron flow from the discharge plasma to the anode. Different magnetic field configurations (divergent, cusped, multipole, etc.) can be created by routing the anode wire in various ways through the discharge chamber. The thruster is also designed so ion currents to various internal surfaces can be measured directly. This allows the determination of the distribution of ion currents within the discharge chamber. Experiments indicate that the distribution of ion currents is strongly dependent on the shape and strength of the magnetic field but independent of the discharge current, discharge voltage, and neutral flow rate. Measurements of the energy cost per plasma ion indicate that this cost decreases with increasing magnetic field strength due to increased anode shielding from the primary electrons. Energy costs per argon plasma ion as low as 50 eV were measured. The energy cost per beam ion was found to be a function of the energy cost per plasma ion, extracted ion fraction, and discharge voltage. Part of the energy cost per beam ion goes into creating many ions in the plasma and then extracting only a fraction of them into the beam. The rest of the energy goes into accelerating the remaining plasma ions into the walls of the discharge chamber. Measurement of ion fluxes across a virtual anode surface appears to indicate that ions cross this surface with velocities approaching their random thermal velocity rather than the Bohm velocity.

Nomenclature

A	= area, m^2
B	= magnetic flux density, T
E	= electron energy, eV
e	= electronic charge, C
f	= extracted ion fraction
J	= current, A
k	= Boltzmann's constant = 1.38×10^{-23} J/K
m	= mass, kg
n	= plasma density, m^{-3}
P	= specific power, eV/ion
r	= radial position, m
T	= temperature, K
v	= velocity, m/s
V	= voltage, V
μ_0	= permeability constant = 1.26×10^{-6} H/m

Subscripts

B	= beam
b	= Bohm
back	= back surface of discharge chamber
D	= discharge
E	= emission
e	= electron
f	= magnetic field
i	= ion
P	= production or plasma
S	= virtual anode surface
side	= side surface of discharge chamber
screen	= screen grid
w	= all thruster cathode potential surfaces

Presented as Paper 82-1936 at the AIAA/JSAASS/DGLR 16th International Electric Propulsion Conference, New Orleans, La., Nov. 17-19, 1982; submitted Dec. 10, 1982; revision received April 25, 1983.

*Research Assistant, Department of Mechanical Engineering. Student Member AIAA.

†Professor, Department of Mechanical Engineering. Member AIAA.

Introduction

A GREAT deal of effort has been expended over the last two decades on research to improve the efficiency of electron-bombardment ion thrusters. Much of this effort has centered on the containment of the high energy or primary electrons in the main discharge region of the thrusters, and has resulted in a rather interesting evolution of the thruster magnetic field configurations.[1,2] In spite of this effort, the energy cost per beam ion (in electron volts) for most thrusters is still on the order of 15 to 30 times the first ionization potential energy of the propellant atom.‡ For example, the *J*-series thruster[3] using mercury, operates with a discharge power of 190 eV/beam ion at a beam current of 2 A and a 32-V discharge. This is a factor of 18 greater than the first ionization potential for mercury. For SERT II,[4] this factor is about 20. Ramsey's magnetoelectrostatic thrusters[5] typically operate with factors of 16 for both argon and xenon as did Sovey's argon line-cusp thruster.[6] Multipole thrusters of Isaacson[7] (using xenon) and Longhurst[8] (using mercury) operated with discharge power losses around 18 and 26 times the respective ionization potentials.

Dugan and Sovie[9] have shown that the energy required to produce an argon ion in plasmas similar to those commonly found in ion thrusters should be on the order of 50 eV. That this energy is greater (by approximately a factor of 3) than the ionization potential is due primarily to the fact that the ionization process is accompanied by some excitation of the neutral atoms. Inherent in this analysis is the assumption that electrons lose energy through inelastic collisions with the neutral atoms exclusively, i.e., that electron energy losses to the walls are negligible. In the case of ion thrusters, this condition is approximately satisfied when the primary electrons are prevented from reaching the anode by a magnetic field and when only low-energy electrons are removed from the plasma at the anode. Thus it should be expected that a properly designed ion thruster (i.e., one which prevents primary electrons from having direct access to the

‡For operation at the "knee" of the discharge power-propellant utilization curve.

anode) would produce argon ions in the plasma at an approximate energy cost of 50 eV.

This suggests that the high energy-cost per beam ion of typical thrusters is not the result of inefficient plasma ion production, but rather it is the result of the fact that the fraction of these ions being extracted into the beam is substantially less than unity. If every ion produced in the plasma was extracted into the beam, the thruster would be operating at a discharge power level of 50 eV/beam ion (50 W/beam A). This is probably the maximum energy efficiency that could be expected for an argon thruster.

To approach this maximum efficiency one must understand the behavior of, and be able to control, the ion currents inside the discharge chamber. The flexible magnetic field thruster was developed to study the behavior of these ion currents. The unique features of this thruster are that it allows drastic changes in its magnetic field configuration to be accomplished quickly and easily, and that it is designed so ion currents can be measured to its various interior surfaces.

Changes in magnetic field configuration are made possible through the use of a copper wire anode through which a direct current on the order of 100 A is passed. This current sets up a circumferential magnetic field around the anode. The anode wire may then be bent into any shape inside the discharge chamber to produce the magnetic field configuration of interest. Axial, mildly divergent, strongly divergent, cusped, and multipole magnetic field configurations have all been created with this thruster.

This paper provides a detailed description of the flexible magnetic field thruster design and some of the results obtained with it. These results include the measurement of ion currents to all thruster cathode potential surfaces. From these data, the total ion production rate, energy cost per plasma ion and extracted ion fraction were calculated. In this study, these performance parameters were monitored as the magnetic field configuration and strength, discharge current, discharge voltage, and neutral flow rate were varied.

Apparatus and Procedure

The primary feature of the flexible magnetic field thruster is the anode. It is made from a 3.2-mm-diam. copper tube through which a relatively large direct current is passed. In designing the thruster, the magnitude of the currents needed to produce fields that will prevent primary electrons from reaching the anode surface were first computed to insure they would be reasonable. This was done by recognizing that the magnetic flux density B at a radius r from the centerline of a wire carrying a current J_f is given by

$$B=\mu_0 J_f/2\pi r \tag{1}$$

where μ_0 is the permeability of free space. It has been assumed in writing this equation that the radius r where the field is sought is greater than the wire radius r_0. In order to prevent collection of electrons having an energy E_e (in electron volts), Isaacson found the following condition on the integral of the magnetic flux density had to be satisfied in a similar geometrical situation[10]:

$$\int_{r_0}^{r_1} B\,dr \geq 6.74\times 10^{-6}\sqrt{E_e} \tag{2}$$

In this expression, r_1 is either the radius at which the magnetic flux density drops to a negligible value or the radius at which electrons are injected into the magnetic field, whichever is less. Combining Eqs. (1) and (2) and performing the indicated integration, one can solve for the current required through the wire. After substituting for the permeability one obtains

$$J_f=\frac{33.7\sqrt{E_e}}{\ln(r_1/r_0)} \tag{3}$$

For 40-eV primary electrons, a 1.6-mm-radius wire, and a radius of electron injection in the radius range of 1-2 cm, the required magnetic field current given by Eq. (3) is about 100 A. This is large, but not unacceptably so. For a 1.6-mm-radius anode of the order of a meter in length, further analysis suggests that copper can carry the required current with a small voltage drop over the 1-m tube length (~0.1 V) as long as the wire is maintained at a sufficiently low temperature (~80°C). Computations suggest this temperature can be maintained by using a commercially available 3.2-mm-diam copper tube and circulating water through it at a flow rate of a few tens of ml/min.

The basic stainless steel, sheet metal chamber used to house the anodes in this study is shown schematically without an anode in Fig. 1d. For all of the data presented here, this chamber was 17 cm in diameter and 12 cm long. The other sketches in Fig. 1 show perspective cutaway views of anode configurations examined in this study. The magnetic field shapes produced by these windings are also shown. The refractory wire cathode used in the tests was positioned 2.5 cm upstream of the grids in the manner suggested in Fig. 1d for all anode configurations. The cathode employed 0.25-mm-

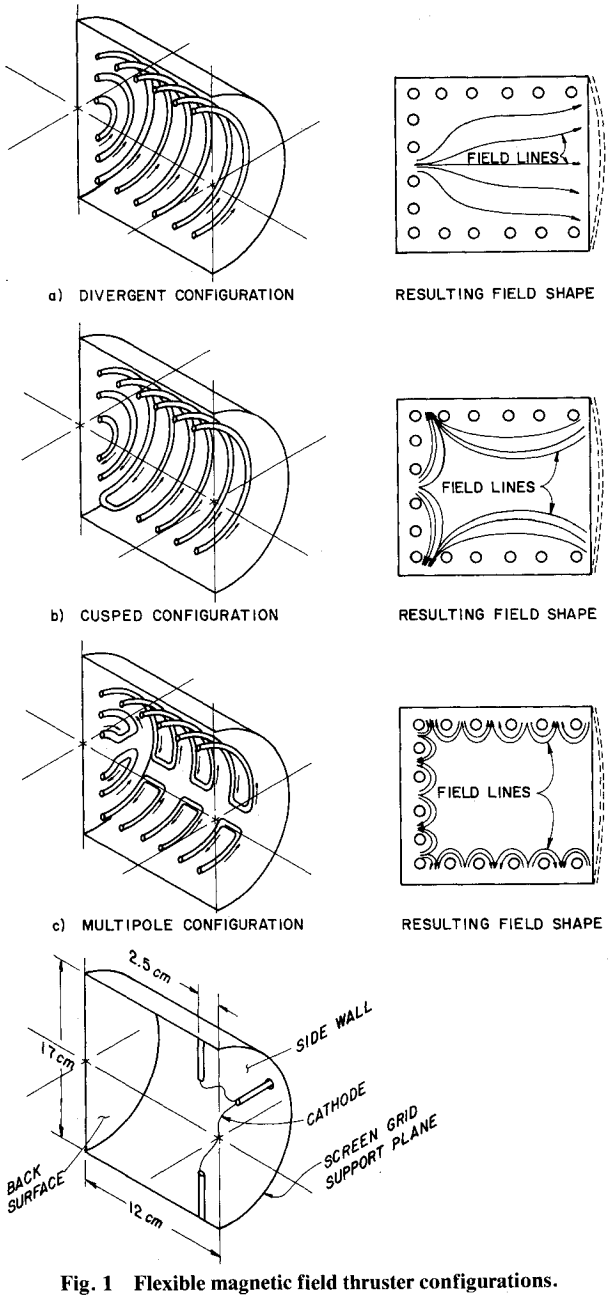

Fig. 1 Flexible magnetic field thruster configurations.

diam tungsten wire about 30 cm in length. This wire was heated using alternating currents in the range 12-15 A from a center-tapped power supply. Argon propellant was used because of the ease with which flow rates could be set and maintained. Tests were conducted at flow rates of 740, 1270, and 1580 mA equivalent. Thruster performance was measured at discharge voltages through the range 30-50 V above the cathode center tap potential. The discharge current was adjusted through the range 2-6A by controlling the alternating current through the refractory cathode.

The grids used in the tests had a 67% open area screen and a 30% open area accelerator. They were operated at a total accelerating voltage of 1500 V and a net-to-total accelerating voltage ratio of 0.67 with a cold grid spacing 0.75 mm. Beam neutralization was accomplished using a refractory wire cathode. All tests were conducted in a 1.2-m-diam × 4.6-m-long vacuum test facility.

To facilitate the measurement of ion currents to various thruster surfaces, the following features were incorporated into the design of the discharge chamber. The thruster back surface, cylindrical side wall, screen grid, and cathode were all electrically isolated from each other. The positive high voltage was connected directly to the cathode center tap. The back surface, side wall, and screen grid were connected to this point through 1-Ω resistors and through a power supply that was used to bias these surfaces negative of cathode potential. During thruster operation, these surfaces could be biased to −70 V (relative to cathode potential). At this bias, electron collection on these surfaces was eliminated and the ion current to each surface could be determined by measuring the voltage drop through each resistor. It is noted that ion currents going to the anode surface and recombining there are not counted when measurements are made in this way. Due to the difficulty of measuring the ion current to the anode surface it was decided to treat the ion-electron recombination there as if it were a volume recombination process. That is, the energy lost as a result of ion neutralization at the anode surface was included in the overall average energy cost to produce a plasma ion.

By measuring the ion current to the thruster body and screen grid in the manner suggested above one is provided with a powerful tool for evaluating thruster performance. It is really an extension of the Langmuir probe technique proposed by Sovey[6] and is essentially the same approach used by Siegfried in studying hollow cathodes.[11] In this case, however, the back surface, side wall, and screen grid act as probes. The value of the measurement lies in the fact that the sum of the body and screen grid ion currents represents the current of ions produced in the chamber but not extracted through the grids. The sum of this current and the beam current is the total ion production rate (expressed as a current). Knowing this total ion production rate, one can compute the fraction of ions produced that are extracted (beam current-to-total production rate ratio) and the energy cost of a plasma ion. The first of these parameters indicates the efficiency of the discharge chamber in directing ions through the grids; the second, the efficiency of the discharge chamber electrons in producing ions.

It should be noted that when measurement of the total ion production rate is made by summing the ion currents to each negatively biased surface, the measured value is less than the actual value because the ion current to the anode surface has not been included. Further, the energy cost per plasma ion based on the measured ion production rate will be greater than the actual value. The measured values of both the ion production rate and the energy cost per plasma ion will approach the actual values as the physical anode area decreases. In these tests, the anode area exposed to the plasma was the same for each of the configurations of Fig. 1. Thus the error in the measured values of these parameters should be approximately the same in each case, and meaningful comparisons can be made between the different magnetic field configurations. Finally, it is believed that the ion current density to the anode is small compared to the ion current density to the negatively charged surfaces due to the difference in ion velocities to each surface. Thus the errors between the measured and actual values should be relatively small.

Applying a large negative bias to the various discharge chamber surfaces did not significantly alter the discharge chamber operation. When the bias was applied, the current to each surface rose from zero (at floating potential) to the value corresponding to the ion current being collected. As the negative bias on a surface was increased, the discharge and beam currents would also increase. The discharge current increase was caused by the collection, at the anode, of additional electrons that had previously neutralized the ions at the walls by coming directly from the plasma. When the negative bias was applied, these electrons could no longer neutralize the ions at the walls directly from the plasma, but rather they had to be collected by the anode and then be passed through the discharge power supply so they could reach the walls. The beam current increase associated with biasing discharge chamber surfaces is a result of the increase in discharge current brought on by the phenomenon just described. In conducting the tests it was found that when the discharge current was restored to its original value the beam current would also return to its original value. This indicates that the thruster discharge chamber efficiency was the same, regardless of whether the back, side, and screen surfaces were allowed to float, or were biased strongly negative of cathode potential—provided the discharge current was held constant. At first glance, this is a rather remarkable result. In the floating case, the ions reaching the walls are neutralized there by high-energy electrons from the plasma. In the other case, the ions are neutralized by electrons from the discharge supply which are primarily low-energy electrons collected by the anode and then pumped up to the discharge chamber surface potential through the anode power supply. That these two conditions should result in identical discharge chamber efficiencies required an explanation.

With the walls floating, the discharge current J_D is the sum of the cathode emission current J_E and the beam current J_B, so that

$$J_D = J_E + J_B \tag{4}$$

In this case the ions are neutralized at the walls by high-energy electrons emitted by the cathode. When the walls are biased sufficiently negative of the cathode potential so that no electrons from the plasma can reach them, the discharge current becomes

$$J_D = J'_E + J_B + J_W \tag{5}$$

where J_W is the magnitude of the ion current to the walls—a current that remains unchanged as the walls are biased negatively. Now if the discharge currents of Eqs. (4) and (5) are to be made equal, and if at this condition the beam currents are equal, than the cathrode emission J'_E in Eq. (5) must be decreased by an amount equal to J_W. That is, the rate at which high-energy electrons are injected into the plasma for the case where the walls are biased negatively, must be reduced by an amount exactly equal to the rate at which high-energy electrons were lost to the walls in the first case. This results in the density of high-energy electrons being the same in both cases, and since everything else was held constant, the efficiency must be unchanged.

Results and Discussion

Existing Thruster Designs

In the first part of this study, three thruster magnetic field configurations were examined: the divergent field, the single cusped field, and the multipole configuration. Each of these

configurations was easily created with the flexible field thruster. Figure 1 shows these configurations and how the anode wire must bend in order to create each particular magnetic field shape. In each of these three configurations, the loop separation was approximately 2 cm and the total anode length exposed to the plasma was 280 cm. In addition, the volume and surface area of the region bounded by the anode was the same for each configuration. The effect of increasing the magnetic field strength for the divergent field thruster configuration is illustrated in Fig. 2. In this figure, the fractions of total ion current produced (J_p) which go to: the back surface (J_{back}/J_p), the side wall (J_{side}/J_p), the screen grid (J_{screen}/J_p), and the beam (J_B/J_p) are plotted as functions of normalized magnetic field current through the anode wire. These data were taken at a discharge current of 2.0 A, a discharge voltage of 50 V, and a neutral flow rate of 1580 mA eq. However, it was found that the ion current distribution in the discharge chamber was independent of discharge current, discharge voltage, and neutral flow rate over the ranges investigated. Because of this independence from discharge conditions, the curves shown in Fig. 2 can be considered generally applicable to the divergent magnetic field configuration. Examination of Fig. 2 indicates that the fraction of the total ion current extracted into the beam increases with increasing field current. In addition, the fractions of the total ion current going to the back surface and screen grid increase slightly, while that to the side wall decreases. This is clear evidence that the magnetic field strength can influence the distribution of ion currents inside the discharge chamber. The decrease in the fraction of ion current to the side wall is believed to be primarily the result of a radial plasma density distribution in the discharge chamber that becomes increasingly nonuniform as the field current is increased. Most of the ion current going to the back surface is assumed to be going there through the "hole" in the magnetic field on the centerline of the thruster.

The distribution of ion currents for the cusped field thruster (Fig. 1b) configuration is shown in Fig. 3. Again, the fractions of ion currents to each surface are plotted against the normalized magnetic field current. Here the same basic trends exhibited by the divergent field configuration are seen. However, in this case the redistribution of ion currents is less pronounced than in the previous case. This appears to indicate that the plasma density remains more uniform at high field strengths in the cusped configuration than in the divergent field geometry. This plasma uniformity is also reflected in the respective ion beam profiles, which are more uniform in the cusped field configuration than they are for the divergent one.[2] It is believed that an additional factor that causes the side wall current fraction to be higher for the cusped configuration than for the divergent one is the plasma leakage that occurs at the cusp.

Finally the distribution of currents for the multipole configuration (Fig. 1c) is shown in Fig. 4. Here, interestingly enough, the magnetic field strength has no effect on the gross distribution of ion currents inside the discharge chamber. Further, the fractions of current to each surface was found to be exactly equal to the area of that surface divided by the total area of the primary electron region. This was true only at zero field current for the first two configurations. This appears to indicate that the ions move toward the walls with nearly equal probability in all directions in a multipole thruster. It should be noted here that this result applies only to low field strength multipole thrusters. It was not possible to create the 0.3 T magnetic fields now found at the pole pieces of some multipole designs.[12] The improved performance of these designs suggests that some redirection of ion currents is indeed occurring. In any case, the uniform ion current distribution of low field strength multipole thrusters is clearly demonstrated here. The fact that ions are lost uniformly in all directions from the plasma implies that the extracted ion fraction should always be less than 50% for multipole thrusters of low field strength design.

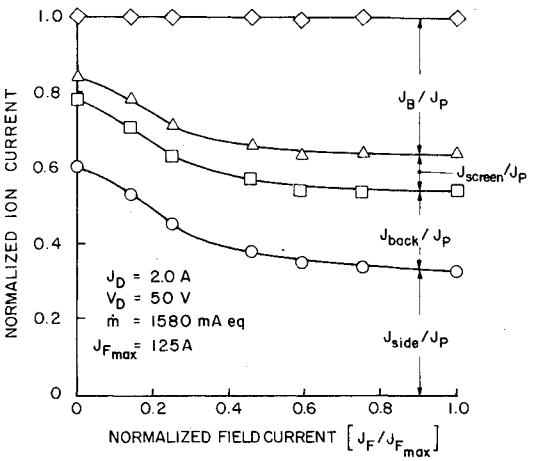

Fig. 2 Ion current fractions to discharge chamber surfaces for the divergent field configuration.

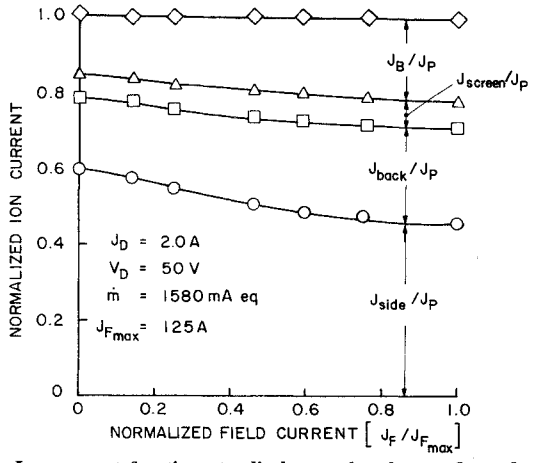

Fig. 3 Ion current fractions to discharge chamber surfaces for the cusped field configuration.

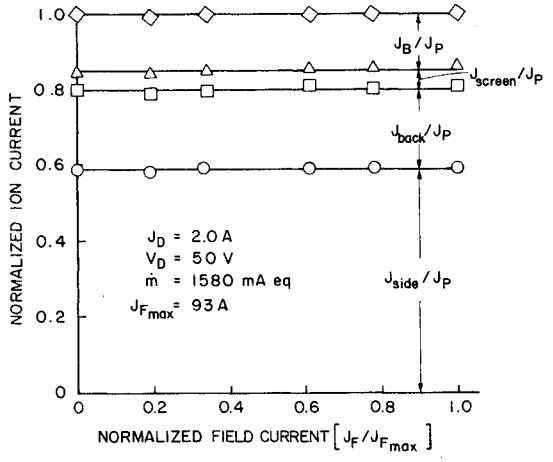

Fig. 4 Ion current fractions to discharge chamber surfaces for the multipole field configuration.

For comparison purposes, the fraction of ions directed toward the grids, $(J_B+J_{screen})/J_p$, is plotted against the magnetic field current in Fig. 5 for the three thruster configurations. The advantage of the divergent field geometry in terms of the fraction of ions directed toward the grids is clear.

Plasma Ion Production

The energy required to create an ion in the plasma has, as one would expect, a strong influence on the overall thruster

efficiency. The relationship between this energy cost per plasma ion and that per beam ion can be related using quantities measured in the tests described in this paper. The energy cost per plasma ion (P_p, in electron volts) is defined by

$$P_p = \frac{(J_D - J_p) V_D}{J_p} \tag{6}$$

where V_D is the discharge voltage. The ion production rate J_p can be approximated as the sum of the beam current and ion current to the discharge chamber walls J_W, i.e.,

$$J_p = J_B + J_W \tag{7}$$

Substituting Eq. (7) into Eq. (6) yields

$$P_p = \frac{[J_D - (J_B + J_W)] V_D}{J_B + J_W} \tag{8}$$

This can be rewritten as

$$P_p = \frac{(J_D - J_B) V_D}{J_B} \left(\frac{J_B}{J_B + J_W}\right) - \frac{J_W V_D}{J_B} \left(\frac{J_B}{J_B + J_W}\right) \tag{9}$$

Recognizing that $(J_D - J_B) V_D / J_B$ is the discharge power P_D (in eV/beam ion), and letting f be the extracted ion fraction defined by

$$f = J_B / (J_B + J_W) \tag{10}$$

then, Eq. (9) can be written in the form

$$P_D = \frac{P_p}{f} + \frac{(1-f) V_D}{f} \tag{11}$$

This is the desired relation between the energy cost per plasma ion and the energy cost per beam ion. The first term on the right-hand side of this equation reflects the energy lost because ions are produced that recombine on the walls and are not extracted into the beam. The second term represents the energy used to accelerate the plasma ions that go to the walls of the discharge chamber into these surfaces.

The plasma ion energy cost has been determined for each thruster configuration and at each operating point considered in this study using Eq. (6). A sample of the results obtained with the cusped field thruster are shown in Fig. 6. These data indicate that the energy cost per plasma ion decreases with increasing magnetic field strength (due to increased anode shielding from primary electrons). In addition, it indicates that the cost increases with discharge current and decreases with neutral flow rate. However, it is relatively independent of discharge voltage. While these data were obtained with the cusped field configuration, results obtained with the other thrusters showed similar trends. These and other data indicate that the energy cost per plasma ion can be made as low as 50 to 60 eV for the argon propellant used.

In the course of measuring the total ion production rate it was noticed that this rate was frequently much greater than the neutral flow rate in equivalent milliamperes. An example of this is shown in Fig. 7 for data collected on the cusped field thruster. The ion production rate being greater than the neutral flow rate is an indication that the walls of the discharge chamber behave as a virtual source of propellant atoms. Also shown on this figure is the beam current. This figure indicates rather dramatically how the ion production rate can be significantly greater than the neutral flow rate,

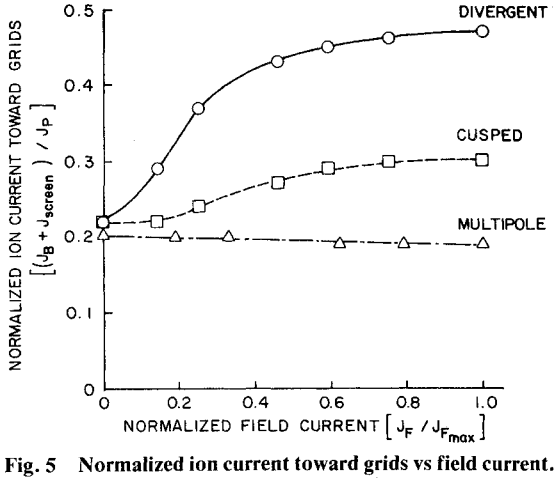

Fig. 5 Normalized ion current toward grids vs field current.

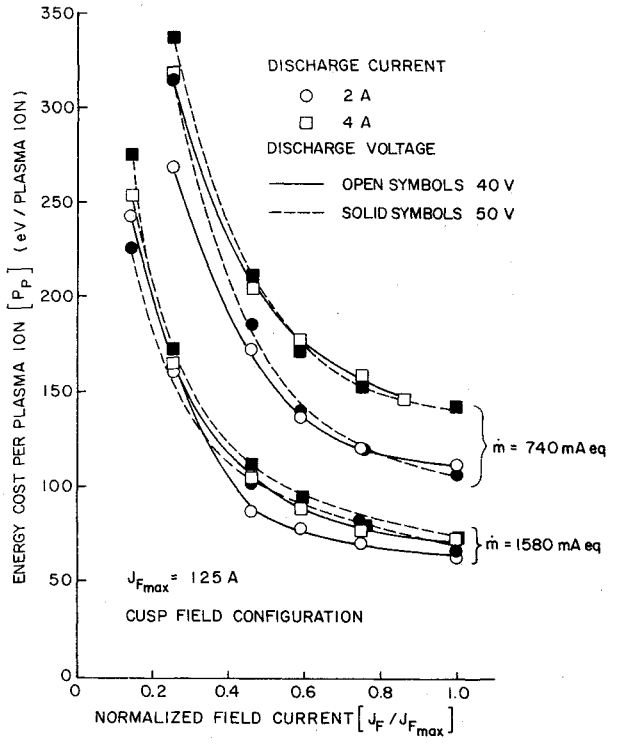

Fig. 6 Plasma ion energy cost in the cusped field configuration.

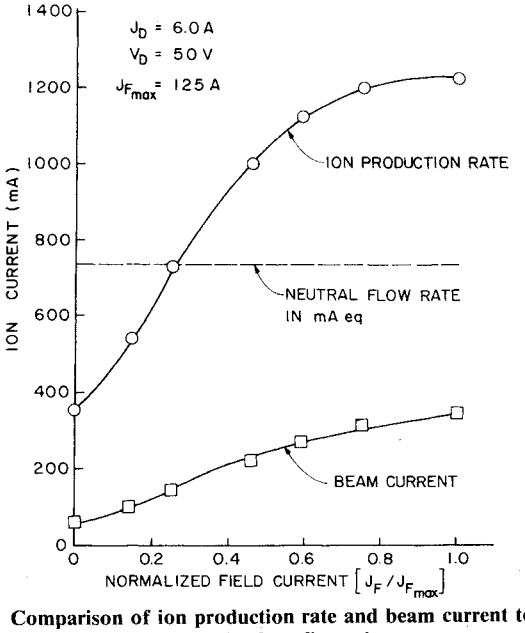

Fig. 7 Comparison of ion production rate and beam current to the neutral flow rate for the cusped field configuration.

and yet the beam current is still substantially less than the flow rate. This does not mean, however, that if every ion produced could be extracted into the beam that one would get a beam current greater than the flow rate. Instead, the neutral density would decrease, causing a corresponding decrease in the ion production rate such that the beam current (assuming only singly charged ions) would always be less than the neutral flow rate.

Other Considerations

In addition to the tests described above, several other configurations of the flexible field thruster were tested in an effort to reduce ion losses to the walls still further. The number and type of configurations that can be tested is limited only by the imagination of the researcher. To date, no configuration of the flexible field thruster has directed a greater fraction of ions toward the grids than the divergent field configuration. However, in the course of this effort a very interesting phenomenon was observed. Tests were being run on the flexible field thruster in an axial magnetic field configuration, as shown in Fig. 8. In addition to the solenoidal anode the thruster was equipped with an external solenoid. This allowed the magnetic field in the discharge chamber to be created by 1) passing a current through the anode wire only; 2) passing a current through the external solenoid only; or 3) passing currents in opposing or adding directions through both wires simultaneously to produce a wide range of magnetic field conditions. With this thruster configuration it was observed that at any given flow rate, discharge current and discharge voltage, the ion current to the side wall was smaller when the magnetic field was created with the external solenoid alone than it was when a magnetic field of identical strength was created with the internal solenoid alone. This indicates that the plasma is being contained better when the magnetic field is created by the external solenoid than it is when the internal anode wire is used. Why this should occur was not immediately apparent.

The reason the external coil gives better performance than the internal one can be understood, however, by considering Fig. 8 further. Figure 8a shows the magnetic field lines for the case where the field is produced entirely by passing a current through the anode wire. Figure 8b shows the field lines when the field is produced entirely by the external solenoid. The anode wire in this second case serves only as the anode. In Fig. 8b, we notice that certain field lines intercept the anode surface directly. As we progress outward from the centerline of this thruster along a radius, the surface of revolution of the first field line that we encounter which intercepts the anode surface is called the virtual anode surface. It is so called because once an electron becomes attached to a field line on this surface it has a high probability of being collected by the anode. Consequently, few electrons would be expected to be found at radial locations greater than that of the virtual anode surface. This in turn implies that the plasma density should be reduced substantially in the region outside of this surface. It appears that the reduced ion flux to the side wall is a result of the reduced plasma density in this region. For the case of Fig. 8a (magnetic field created by the internal solenoid), however, it is seen that no field lines intercept the anode directly; instead, they tend to form concentric circles around the anode wire. Consequently there is no virtual anode surface. Further, the field strength between adjacent turns of the anode wire goes to zero. These two factors apparently enable the plasma to leak out of the volume bounded by the anode wire, and the result is an ion current to the side wall greater than that observed with the external solenoid.

When the virtual anode surface is present, as mentioned earlier, ion losses to the side wall can be greatly reduced. It was postulated that this reduced ion loss to the wall was the result of a greatly reduced plasma density adjacent to it.

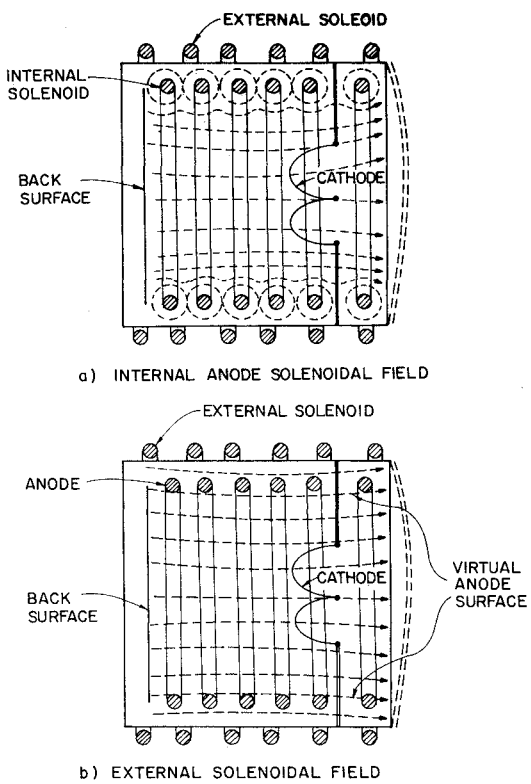

Fig. 8 Axial magnetic field thruster configurations.

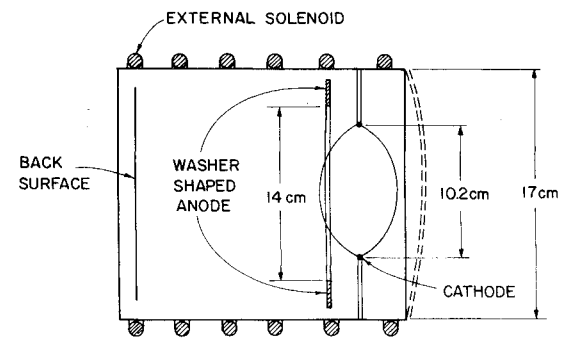

Fig. 9 Axial magnetic field thruster with "washer-shaped" anode.

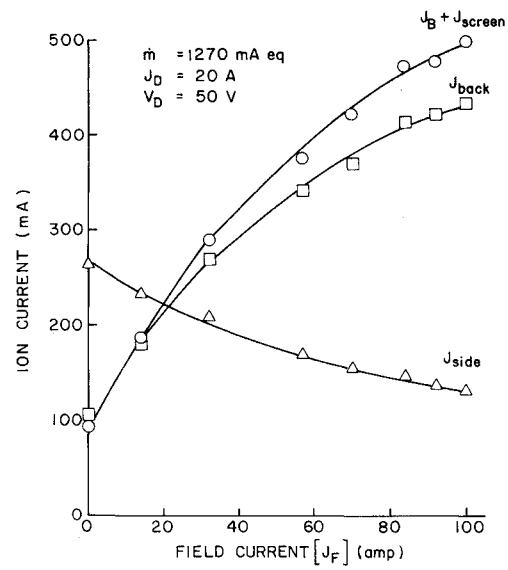

Fig. 10 Ion currents to discharge chamber surfaces for the axial field thruster with "washer-shaped" anode.

Further, this reduction in plasma density was believed to occur across the virtual anode surface because of the removal of electrons from the plasma by the anode. If this is indeed the case, that is, if the plasma density is reduced dramatically across the virtual anode surface, then the ions must cross this surface with an average velocity substantially less than the Bohm[13] velocity. This must be so, for if the ions crossed this surface from a region of high density to a region of low density with the Bohm velocity, then an excess of positive charge would very quickly be built up in the low-density region. This excess charge would serve to reduce the ion velocity across the virtual anode surface to the point where the flux of positive charges across the surface was consistent with the condition of quasicharge neutrality in both the high- and low-density regions.

To see if this was indeed the case, the following experiment was performed. A thruster having the configuration shown schematically in Fig. 9 was constructed. The anode consisted of a washer-shaped piece of 0.025-cm-thick stainless steel. An axial magnetic field was created in the discharge chamber through the use of a six turn solenoid wrapped around the cylindrical thruster body. The cathode consisted of a tungsten wire bent into a circle 10.2 cm in diameter. With this configuration, the entire side wall was protected by the virtual anode surface, but the physical anode area exposed to the plasma was extremely small compared to the total surface area bounding the plasma. This allowed the ion current to the side wall to be measured very accurately, since the ion current to the physical anode was negligible. The actual ion currents to each thruster surface are shown in Fig. 10 for an argon flow rate ($\dot{m}$) of 1270 mA, a discharge current (J_D) of 2.0 A, and a discharge voltage (V_D) of 50 V. It is noteworthy that this discharge chamber gave a higher extracted ion fraction than the divergent field design (Fig. 1a and Fig. 5). The remarkable aspect of the results of Fig. 10 is, however, that as the ion current toward the grids ($J_B + J_{screen}$) increases by approximately a factor of 5, due to an increase in the magnetic field current from 0 to 100 A, the ion current to the side wall actually decreases. This shows that the virtual anode surface does a remarkable job of containing the plasma. It is believed that this occurs because ions cross this surface with velocities approaching their random thermal velocity rather than the Bohm velocity. The following rough calculation supports this hypothesis.

Assuming that the ions reach the accelerator system with the Bohm velocity based on an estimated electron temperature of 5 eV, the plasma density just inside of the virtual anode surface was estimated from an ion beam current density profile to be 2.4×10^{-16} m^{-3}. If the ions crossed the virtual anode surface with the Bohm velocity, then the current to the side wall would be given by the formula,

$$J_{side} = neA_s v_b \tag{12}$$

where n is the plasma density (just cited); e is the charge for singly charged ions in coulombs; A_s is the area of the virtual anode surface; and v_b is the Bohm velocity corresponding to an electron temperture (T_e) of 5 eV. If, on the other hand, the ion current depends on the ion random thermal velocity, then

$$J_{side} = \tfrac{1}{4} neA_s \langle v \rangle \tag{13}$$

where

$$\langle v \rangle = \sqrt{8kT_i/\pi m_i} \tag{14}$$

and T_i is the ion temperature (assumed to be equal to 600 K); k is Boltzmann's constant; and m_i is the ion mass. Using the density cited previously, Eq. (12) gives an ion current to the side wall of 1010 mA, whereas Eq. (13) gives a current of 40 mA. The measured current at the maximum magnetic field was 113 mA. If the one-fourth factor in Eq. (13) is eliminated, then the equation would correspond to the current due to a directed thermal velocity and the result is a current of 160 mA. Admittedly these calculations are somewhat crude, but they are believed to be accurate to better than a factor of 2. On the basis of these results, it is suggested that the ions cross the virtual anode surface with a velocity approaching their thermal velocity rather than their Bohm velocity.

This phenomenon can also be used to explain the low ion flux across the vritual anode surface observed in the SERT II thruster.[14] In this case the average current density across this surface was measured and found to be approximately 15% of the average current density toward the grids. Rough calculations suggest that if the ions have the Bohm velocity at this surface, then the average current density would be on the order of 250% of the average current toward the grids. If they are assumed to have the random thermal velocity, however, the calculated current density is about 10% of the current toward the grids. It appears that the ions do not cross the virtual anode surface with the Bohm velocity. It should be pointed out that these results are still preliminary and final judgment must await detailed probing of the plasma around the virtual anode surface.

In light of this velocity phenomenon, it should be noted that the flexible magnetic field thruster does not produce any virtual anode surfaces regardless of its configuration (for reasons given in connection with Fig. 8). This implies that the flexible field thruster does not imitate exactly those thruster designs which do create virtual anode surfaces. This includes virtually all current designs. However, based on results obtained with the thruster configurations shown in Figs. 8a and 8b, it is believed that the ion flux distributions obtained with the flexible field thruster are still qualitatively correct, and meaningful comparisons can be made between different magnetic field configurations using this technique.

Conclusions

The ability to make drastic changes in magnetic field configurations, together with the ability to measure ion currents to different thruster surfaces, makes the flexible magnetic field thruster a powerful tool for the study of magnetic field configuration effects on thruster operation. With this thruster, it was observed that the distribution of ion currents inside the discharge chamber was strongly dependent on the shape and strength of the magnetic field. This distribution of ion currents, however, was found to be independent of the discharge current, discharge voltage, and the neutral flow rate. With no magnetic field, the ions move to the thruster walls with equal probability in all directions, and the fraction of current to each surface bounding the plasma is equal to the area of that surface divided by the total surface area of the primary electron region.

The fraction of ion current to each thruster surface was found to vary as a function of magnetic field strength for both the divergent and cusped field configurations. Generally, the fraction of ion current to the side wall would decrease and the fraction of ion current toward the grids would increase as the field strength was increased for these configurations. No such redistribution of ion currents was observed for the multipole configuration. In this case, the ion current distribution remained the same as it was for the zero magnetic field condition.

Measurements of the energy cost per plasma ion indicated that this cost decreased with increasing magnetic field strengths. This effect was attributed to increased shielding of the anode from the primary electrons. Energy costs per argon plasma ion as low as 50 eV were measured.

The energy cost per beam ion was found to be a function of the energy cost per plasma ion, the extracted ion fraction, and the discharge voltage. Part of the energy cost per beam ion goes into creating many ions in the plasma when only a fraction of them is extracted into the beam. The rest of the

energy goes into accelerating the remaining plasma ions into the walls of the discharge chamber.

The flexible field thruster does not exactly imitate the discharge chambers of existing thruster designs due to its inability to produce virtual anode surfaces. However, the ion current distributions measured with it are still believed to be qualitatively correct. The virtual anode surface provides a boundary between high- and low-density plasma regions. Ions from the high-density region cross this boundary with velocities approaching their random thermal velocity. This indicates that ion losses from typical ion thruster discharge chambers can be reduced by bounding the plasma with virtual anode surfaces.

Acknowledgment

This work was performed under NASA Grant NGR-06-002-112.

References

[1]Robinson, R.S., "Physical Processes in Directed Ion Beam Sputtering," NASA CR-159567, March 1979.

[2]Beattie, J.R. and Wilbur, P.J., "Cusped Magnetic Field Mercury Ion Thruster," *Journal of Spacecraft and Rockets,* Vol. 14, Dec. 1977, pp. 747-755.

[3]Bechtel, R.T., "The 30 cm J Series Mercury Bombardment Thruster," AIAA Paper 81-0714, 1981.

[4]Kerslake, W.R., Goldman, R.G., and Nieberding, W.C., "SERT II: Mission, Thruster Performance, and In-Flight Thrust Measurements," *Journal of Spacecraft and Rockets,* Vol. 8, March 1971, pp. 213-224.

[5]Ramsey, W.D., "Magnetoelectrostatic Thruster Physical Geometry Tests," *Journal of Spacecraft and Rockets,* Vol. 19, March 1982, pp. 133-138.

[6]Sovey, J.S., "Performance of a Magnetic Multipole Line-Cusp Argon Ion Thruster," *Journal of Spacecraft and Rockets,* Vol. 19, May-June 1982, pp. 257-262.

[7]Isaacson, G.C. and Kaufman, H.R., "15-cm Multipole Gas Ion Thruster," *Journal of Spacecraft and Rockets,* Vol. 14, Aug. 1977, pp. 469-473.

[8]Longhurst, G.R. and Wilbur, P.J., "15-cm Mercury Multipole Thruster," *Journal of Spacecraft and Rockets,* Vol. 16, Jan.-Feb. 1979, pp. 42-47.

[9]Dugan, J.V. and Sovie, R.J., "Volume Ion Production Costs in Tenuous Plasmas: A General Atom Theory and Detailed Results for Helium, Argon, and Cesium," NASA TN D-4150, 1967.

[10]Isaacson, G.C., "Multipole Gas Thruster Design," NASA CR-135101, June 1977.

[11]Siegfried, C.E., "A Phenomenological Model Describing Orificed Hollow Cathode Operation," *Ion and Advanced Electric Thruster Research—1980,* NASA CR-165253, Dec. 1980.

[12]Sovey, J.S., "Improved Ion Containment Using a Ring-Cusp Ion Thruster," AIAA Paper 82-1928; see also NASA TM-82990, 1982.

[13]Bohm, D., "Minimum Ionic Kinetic Energy for a Stable Sheath," *The Characteristics of Electrical Discharges in Magnetic Fields,* edited by A. Guthrie and R.K. Wakerling, McGraw-Hill, New York, 1949, pp. 77-86.

[14]Wilbur, P.J., "Advanced Space Propulsion Thruster Research," NASA CR-165584, Dec. 1981, p. 82.